Vol 14 No 7, July 2005
1009-1963/2005/14(07)/1423-05

Chinese Physics

© 2005 Chin. Phys. Soc.
and IOP Publishing Ltd

Calculation of incident ion distribution in a rectangular hollow cathode in magnetic field

Fang Tong-Zhen(房同珍)†, Zhang Long(张 龙), and Wang Long(王 龙)

Institute of Physics, Chinese Academy of Sciences, Beijing 100080, *China*

(Received 25 November 2004; revised manuscript received 5 April 2005)

Incident ion distribution inside a rectangular hollow cathode in a uniform magnetic field is studied analytically. The analysis shows that the ion distribution on one sidewall is not interfered by the other sidewall when the depth and width of the cathode are equal, and the ion distribution on the bottom surface related to the depth of the cathode and the number of ions on the bottom surface decrease monotonically from the centre to the sidewall.

Keywords: hollow cathode discharge, incident ion distribution, magnetic field
PACC: 5280Y, 5290

1. Introduction

In classical theory of glow discharge, ions from plasma move across the cathode sheath and hit the cathode, knocking out secondary electrons from the surface. These secondary electrons ionize or excite background gas, generating a negative glow (NG) region. In a hollow cathode discharge, the NG region is enclosed in the cathode. There is a thin sheath around the inner cathode surface in the hollow cathode discharge.[1] The secondary electrons are accelerated through the sheath, and then reflected between the two sheaths of sidewalls while ionizing the gas within the hollow cathode.[2] The ionization in the cathode is enhanced, but the electrons also lose much energy there. Generally the hollow cathode is narrow and deep, the electrons lose much energy in the ionization within the cathode, and a positive column covers the entire region between the electrodes. That is the case of the hollow cathode regime.[3] In contrast, a shallow hollow cathode with a large opening will not trap the electrons in the cathode, but it can provide much more energetic electrons than a deep cathode, and the electron density outside the cathode will also increase. Previous experiments have discovered that the dense sheet plasma is produced by a hollow cathode discharge operating in an enhanced glow regime, which is distinctly different from the abnormal glow or hollow cathode glow regime.[2] The key difference is due to the shallow hollow cathode and the axial magnetic field confinement. The axial magnetic field will help the electrons to form electron beams. If the hollow cathode is narrow and deep, the electrons are reflected between the sheaths many times and lose most of their energy before escaping. As a result, there will be little energetic electron beam. But if the hollow cathode is shallow with a large opening, electrons are reflected only a few times before escaping or escape without reflection between the sheaths, and then form electron beams out of the cathode. Mathew *et al* have reported that a rectangular hollow cathode with width to depth ratio of 1.3–2 can yield a high electron density.[2] Due to the high electron density, this kind of hollow cathode discharge can be used to reflect electromagnetic wave with frequencies below the plasma frequency and serve as a new kind of radar reflector.[4–6]

This article will focus on the ion distribution in a rectangular hollow cathode discharge in an axial magnetic field. This topic has not been studied before so far as we know. The ion distribution in the cathode is important because it determines the secondary electron distribution along the inner cathode surface. And under the action of the axial magnetic field, the spatial distribution of the sheet plasma is mainly determined by the electron distribution in the hollow cathode. Moreover, the electrons emitted from the

†E-mail: tzfang@aphy.iphy.ac.cn

sidewall of the cathode are more important than those from the bottom surface, because they are greatly affected by the magnetic field. Our calculation will give a clear description of the ion distribution in the hollow cathode.

2. Analysis

We suppose that there is a uniform magnetic field along the z-axis and the rectangular hollow cathode is infinite in the y direction, as shown in Fig.1. The depth and width of the rectangular hollow cathode are h and d, respectively. We assume that all ions have the same mass and velocity, and the component of velocity in z axis is denoted as $v_\perp$, the component of cyclotron motion in the xy plane is denoted as $v_{||}$. There is a thin sheath hanging around the outer cathode surface.[2] We consider the ion's movement in the hollow cathode. The ions move along a helical trajectory with a Lamour radius $r_{\rm L}$; and to be simplified, we do not consider the ion–ion collisions and the acceleration in the sheath electric field.

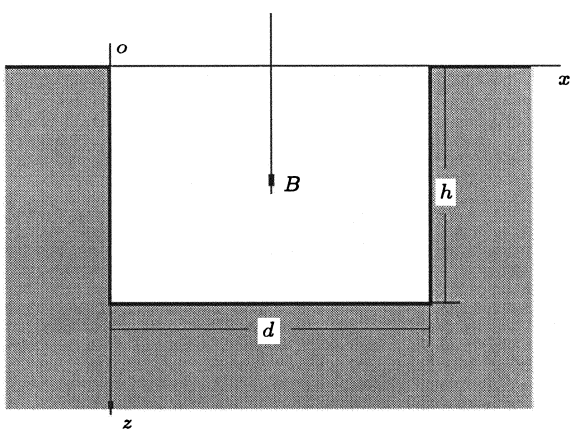


Fig.1. Cross-section of the hollow cathode.

2.1. Distribution along the sidewall

First we assume $r_{\rm L} \leq 2d$, and that the distribution on one sidewall is not affected by the other sidewall. The initial position of the ion is set at the open mouth of the cathode. We suppose that the ions have a cyclotron centre located at x. The initial phase is supposed to be α_0, and the initial position x determines an angle α, as shown in Fig.2, with $\alpha = 2\arccos\left(-\dfrac{x}{r_L}\right)$.

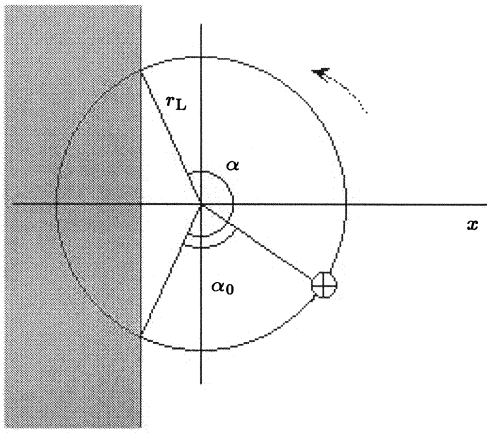


Fig.2. Projection of the ion trajectory on the bottom surface of the cathode.

The time needed for an ion to reach the sidewall is: $t = \dfrac{\alpha - \alpha_0}{v_\perp} r_{\rm L}$. The depth an ion could reach is $z = (\alpha - \alpha_0)\, r_{\rm L} \dfrac{v_{||}}{v_\perp}$. If the cathode is deep enough and α_0=0, the largest depth an ion could reach is $z_{\max} = \alpha r_{\rm L} \dfrac{v_{||}}{v_\perp}$. Suppose that the ion density along the x axis is $n(x)$, and the number of ions with the cyclotron centre in $x \to x + {\rm d}x$ is $n(x){\rm d}x$. The ions are uniformly distributed in the area $(0,\ z_{\max})$ along the sidewall of the hollow cathode. So the ion density along the sidewall is

$$N(x)\,{\rm d}x = \frac{n(x)\,\dfrac{\alpha}{2\pi}}{\alpha r_{\rm L}\dfrac{v_{||}}{v_\perp}}{\rm d}x = \frac{n(x)\,v_\perp}{2\pi r_{\rm L} v_{||}}{\rm d}x. \qquad (1)$$

It is independent of α and z. The total number of ions that hit the area $z \to z + {\rm d}z$ is the integration of $N(x){\rm d}x$ from $x_1 = -r_{\rm L}\cos\dfrac{\alpha}{2}$ to $x_2 = r_{\rm L}$. If $n(x)$ is constant, the integration is easy to carry out,

$$N_z(z) = \int_{x_1}^{x_2} N(x){\rm d}x = \frac{n v_\perp}{2\pi v_{||}}\left[1 + \cos\left(\frac{z v_\perp}{2 r_{\rm L} v_{||}}\right)\right],$$
$$0 \leq z \leq 2\pi r_{\rm L}\frac{v_{||}}{v_\perp}. \qquad (2)$$

Now we can calculate the total number of ions that hit at $(0,\ z)$ on the sidewall:

$$N_{\rm side} = \int_0^z N(z)\,{\rm d}z = \frac{n v_\perp}{2\pi v_{||}} z + \frac{n r_{\rm L}}{\pi}\sin\left(\frac{z v_\perp}{2 r_{\rm L} v_{||}}\right). \qquad (3)$$

If h is longer than $2\pi r_{\rm L}\dfrac{v_{||}}{v_\perp}$, then $N_{\rm side}$ equals $n r_{\rm L}$, which is just half of the number of ions with cyclotron centre located at $(-r_{\rm L},\ r_{\rm L})$ because the other half will hit on the outer side of this sidewall. This is easy to understand from the symmetry.

We have assumed that the cathode is so wide that one sidewall does not interfere the ion distribution on the other sidewall. Now we consider the interference of the other sidewall when $d < 2r_{\mathrm{L}}$, as shown in Fig.3.

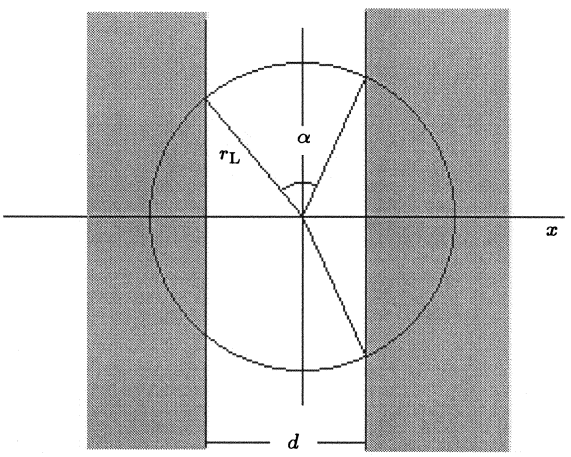


Fig.3. Projection of the ion trajectory on the bottom surface, with $d < 2r_{\mathrm{L}}$.

For the region $z \to z + \mathrm{d}z$ on one sidewall of the cathode, all the ions that hit this region should be divided into two parts. One part is for the ions whose trajectories are not interfered with the other sidewall, and their cyclotron centres lie in $(-r_{\mathrm{L}} \cos \frac{\alpha}{2},\ d - r_{\mathrm{L}})$. The ion distribution for this part of ions is denoted as $N_1(z)$. Then by integrating from $-r_{\mathrm{L}} \cos \frac{\alpha}{2}$ to $d - r_{\mathrm{L}}$, we have

$$N_1(z) = \frac{nv_\perp}{2\pi v_{||}} \left[\frac{\mathrm{d}}{r_{\mathrm{L}}} - 1 + \cos\left(\frac{zv_\perp}{2r_{\mathrm{L}} v_{||}} \right) \right]. \quad (4)$$

The other part, denoted as $N_2(z)$, is for the ions whose trajectories interfere with the other sidewall. This case is more complicated because different z determines different integrated segments. From Fig.3 we can find that $\alpha = \arcsin\left(\frac{x}{r_{\mathrm{L}}}\right) + \arcsin\left(\frac{d-x}{r_{\mathrm{L}}}\right)$, where $\alpha = \frac{zv_\perp}{r_{\mathrm{L}} v_{||}}$, and then we can find x:

$$\begin{aligned} x =& \frac{d}{2} \pm \sqrt{\frac{d^3}{4} - \frac{d^2 - r_{\mathrm{L}}^2 \sin^2 \alpha}{2(1 - \cos\alpha)}} \\ =& \frac{d}{2} \pm \sqrt{r_{\mathrm{L}}^2 \cos^2 \frac{\alpha}{2} - \frac{d^2}{4} \mathrm{ctg}^2 \frac{\alpha}{2}} \\ =& \frac{d}{2} \pm \sqrt{r_{\mathrm{L}}^2 \cos^2\left(\frac{zv_\perp}{2r_{\mathrm{L}} v_{||}}\right) - \frac{d^2}{4} \mathrm{ctg}^2\left(\frac{zv_\perp}{2r_{\mathrm{L}} v_{||}}\right)}. \quad (5) \end{aligned}$$

We define the smaller solution for x as x_1, the larger one as x_2.

When $z \in \left(0, \frac{2r_{\mathrm{L}} v_{||}}{v_\perp} \arcsin \frac{d}{2r_{\mathrm{L}}}\right)$, $N_2(z)$ should be calculated by integrating from $d - r_{\mathrm{L}}$ to r_{L}. When $z \in \left(\frac{2r_{\mathrm{L}} v_{||}}{v_\perp} \arcsin \frac{d}{2r_{\mathrm{L}}}, \frac{r_{\mathrm{L}} v_{||}}{v_\perp} \arccos \frac{d}{2r_{\mathrm{L}}}\right)$, $N_2(z)$ should be calculated by integrating from $d - r_{\mathrm{L}}$ to x_1, finally we obtain

$$N_2(z) = \frac{nv_\perp}{2\pi v_{||}} \left(2 - \frac{d}{r_{\mathrm{L}}}\right)$$

$$\text{for } z \in \left(0, \frac{2r_{\mathrm{L}} v_{||}}{v_\perp} \arcsin \frac{d}{2r_{\mathrm{L}}}\right);$$

$$\begin{aligned} N_2(z) =& \frac{nv_\perp}{\pi v_{||}} \left[1 - \frac{d}{2r_{\mathrm{L}}} \right. \\ & \left. - \sqrt{\cos^2\left(\frac{zv_\perp}{2r_{\mathrm{L}} v_{||}}\right) - \frac{d^2}{2r_{\mathrm{L}}^2} \mathrm{ctg}^2\left(\frac{zv_\perp}{2r_{\mathrm{L}} v_{||}}\right)} \right] \end{aligned}$$

$$\text{for } z \in \left(\frac{2r_{\mathrm{L}} v_{||}}{v_\perp} \arcsin \frac{d}{2r_{\mathrm{L}}}, \frac{r_{\mathrm{L}} v_{||}}{v_\perp} \arccos \frac{d}{2r_{\mathrm{L}}}\right). \quad (6)$$

So the total number of ions that hit the area $z \to z + \mathrm{d}z$ is $N(z) = N_1(z) + N_2(z)$.

For a clear view of the result, we present a simple example here. Figure 4 shows the ion distribution on the sidewall when d=1.5r_{L} and $v_\perp = v_{||}$. The dark area represents the result obtained by considering the interference of the other sidewall, and there is no significant difference between the two distributions. When $d \gg r_{\mathrm{L}}$, and $v_\perp = v_{||}$, we have $\frac{2r_{\mathrm{L}} v_{||}}{v_\perp} \arcsin \frac{d}{2r_{\mathrm{L}}} \approx d$. It means that the interference of the other sidewall could be ignored when the depth and width of the hollow cathode are almost equal.

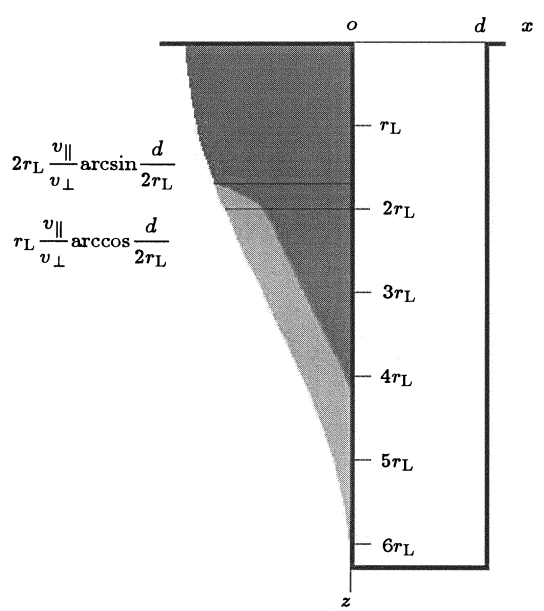


Fig.4. Ion distribution on the sidewall for d=1.5r_{L} and $v_\perp = v_{||}$. The dark area represents the result obtained by considering the interference of the other sidewall.

This result is useful for making Monte Carlo simulation.

2.2. Distribution along the bottom surface

The depth h is important when we consider the ion distribution along the bottom surface. Consider the region $x \to x + \mathrm{d}x$ on the bottom surface of the cathode. We use x' to denote the cyclotron centre of the ions at the open mouth of the cathode, as shown in Fig.5. When $h > 2\pi r_{\mathrm{L}} \dfrac{v_{||}}{v_{\perp}}$, the ions with cyclotron centres $x' > r_{\mathrm{L}}$ could hit the bottom surface. When $h < 2\pi r_{\mathrm{L}} \dfrac{v_{||}}{v_{\perp}}$, the ions with cyclotron centre $x' > -r_{\mathrm{L}} \cos\left(\dfrac{hv_{\perp}}{2r_{\mathrm{L}}v_{||}}\right)$ could hit the bottom surface.

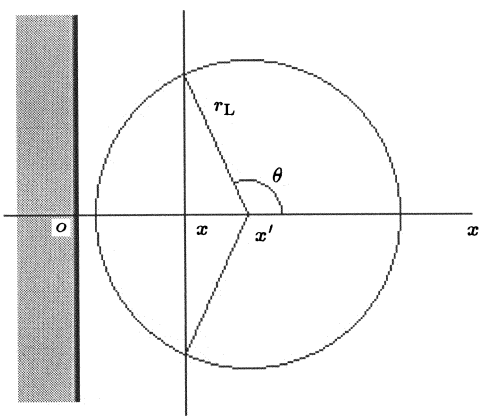


Fig.5. Contribution of ions with cyclotron centres at x' to the density distribution at x on the bottom surface, with $h > z_{\max}$.

The number of ions with cyclotron centre at $(x', x' + \mathrm{d}x')$ is $n\mathrm{d}x'$, where n is also the ion density along the x-axis. The initial positions of these ions are uniformly distributed on the circle shown in Fig.5, so the density on the circle is $n\mathrm{d}x'/2\pi r_{\mathrm{L}}$. We use $N_{\mathrm{ground}}(x)$ to denote the ions that hit $(x, x + \mathrm{d}x)$ on the bottom surface of the cathode, then we obtain

$$\begin{aligned} N_{\mathrm{ground}}(x) &= \int_{r_{\mathrm{L}}}^{r_{\mathrm{L}}+x} 2\frac{n\mathrm{d}x'}{2\pi r_{\mathrm{L}}}\frac{1}{\sin\theta} \\ &= \int_{r_{\mathrm{L}}}^{r_{\mathrm{L}}+x} \frac{n\mathrm{d}x'}{\pi r_{\mathrm{L}}}\frac{r_{\mathrm{L}}}{\sqrt{r_{\mathrm{L}}^2 - (x'-x)^2}} \\ &= \frac{n}{\pi}\arccos\left(1 - \frac{x}{r_{\mathrm{L}}}\right). \end{aligned} \tag{7}$$

Equation (7) shows the distribution on the bottom surface when $h > 2\pi r_{\mathrm{L}} \dfrac{v_{||}}{v_{\perp}}$, and it is valid only for $0 < x < 2r_{\mathrm{L}}$. When $x > 2r_{\mathrm{L}}$, the ion density on the bottom surface is constant, i.e. $N_{\mathrm{ground}}(x) = n$.

Now consider the case of $h < 2\pi r_{\mathrm{L}} \dfrac{v_{||}}{v_{\perp}}$. We denote the ion density on the bottom surface of the cathode as $N'_{\mathrm{ground}}(x)$. In this case, the hollow cathode becomes shallow and more ions can reach the bottom. This means that the integration in Eq.(7) should be changed from $\int_{r_{\mathrm{L}}}^{r_{\mathrm{L}}+x}$ to $\int_{x_0}^{r_{\mathrm{L}}} + \int_{r_{\mathrm{L}}}^{r_{\mathrm{L}}+x}$, where x_0 is determined by h and the ions with cyclotron centres at $x' < x_0$ cannot reach the bottom. The initial phase of all the ions that could hit the bottom must satisfy: $\alpha > \alpha_0$, where $\alpha_0 = \dfrac{hv_{\perp}}{r_{\perp}v_{||}}$ and $\alpha = 2\arccos\left(-\dfrac{x'}{r_{\mathrm{L}}}\right)$ as shown in Fig.6. So it is easy to find that $x_0 = -r_{\mathrm{L}}\cos\left(\dfrac{hv_{\perp}}{2r_{\mathrm{L}}v_{||}}\right)$. x_0 is not marked in Fig.6 because it may be positive or negative.

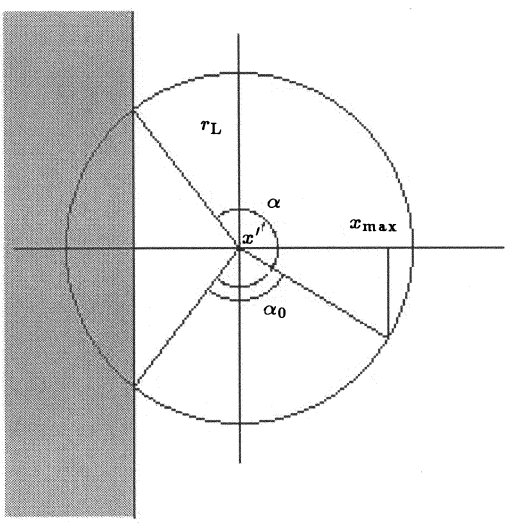


Fig.6. Contribution of ions with cyclotron centres at x' to density distribution on the bottom surface, with $h < z_{\max}$.

We find that $x_{\max}$ is the farthest position on the bottom surface of the hollow cathode that the ions with cyclotron centres in $x' \to x' + \mathrm{d}x$ can reach, and from Fig.6 we can find

$$x_{\max} = x'(1 - \cos\alpha_0) + \sin\alpha_0\sqrt{r_{\mathrm{L}}^2 - x'^2}. \tag{8}$$

When we consider the ions that hit the area $x \to x + \mathrm{d}x$ on the bottom, we should first determine the $x'_{\max}$ by taking x as $x_{\max}$ in Eq.(8). Then we have

$$N'_{\mathrm{ground}}(x) = N_{\mathrm{ground}}(x) + \int_{x_0}^{A} \frac{n\mathrm{d}x'}{\pi r_{\mathrm{L}}}\frac{1}{\sin\theta}, \tag{9}$$

where A represents the smaller one of r_{L} and $x'_{\max}$. The first term on the right side is the contribution of ions with cyclotron centres $x' > 2r_{\mathrm{L}}$, the second term is from the ions with cyclotron centres at $(-r_{\mathrm{L}}, 2r_{\mathrm{L}})$.

3. Conclusion

Our calculation is mainly concerned with the rectangular hollow cathode discharge. The results clearly show the main feature of the ion distribution along the inner surface of the rectangular hollow cathode. Also we find that the ion distribution on one sidewall is not interfered by the other sidewall when the depth and width of the cathode are almost equal. It is helpful to make a Monte Carlo simulation for this kind of hollow cathode discharge, which is useful to produce dense sheet plasma for radar application. Because the secondary electrons emitted from the bottom surface are not affected by the axial magnetic field, they are less important than those from the sidewall. Our calculation also shows that the ion distribution on the bottom surface related to the depth of the cathode and the number of ions on the bottom surface is monotonically decreases from the centre to the sidewall.

References

[1] Manheimer W M, Fernsler R F and Gitlin M S 1998 *IEEE Trans. Plasma Sci.* **26** 1543

[2] Mathew J, Fernsler R F, Meger R A, Gregor J A, Murphy D P, Pechacek R E and Manheimer W M 1996 *Phys. Rev. Lett.* **77** 1982

[3] Liebermann M and Lichtenberg A 1994 *Principles of Plasma Discharges and Materials Processing* (New York: Wiley) p451

[4] Mathew J, Meger R A, Gregor J A, Pechaceck R E, Fernsler R F and Manheimer W M 1995 *IEEE International Radar Conference Record Cat.* No. 95CH-3571-0 742

[5] Meger R A, Mathew J, Gregor J A, Pechaceck R E, Fernsler R F, Manheimer W M and Roboson A E 1995 *Phys. Plasma* **2** 2532

[6] Robson A E, Morgan R L and Meger R A 1992 *IEEE Trans. Plasma Sci.* **20** 1036